Universiteit Antwerpen

This item is the archived peer-reviewed author-version of:

A quantitative method to characterize the Al_4C_3-formed interfacial reaction : the case study of MWCNT/Al composites

Reference:

Yan Laipeng, Tan Zhanqiu, Ji Gang, Li Zhiqiang, Fan Genlian, Schryvers Dominique, Shan Aidang, Zhang Di.- A quantitative method to characterize the Al_4C_3-formed interfacial reaction : the case study of MWCNT/Al composites
Materials characterization - ISSN 1044-5803 - 112(2016), p. 213-218
Full text (Publishers DOI): http://dx.doi.org/doi:10.1016/j.matchar.2015.12.031

uantwerpen.be

Institutional repository IRUA

Accepted Manuscript

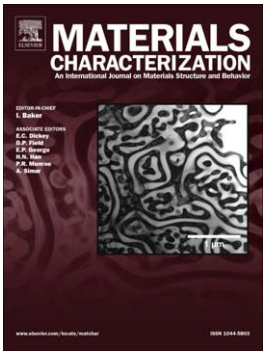

A quantitative method to characterize the Al_4C_3-formed interfacial reaction: the case study of MWCNT/Al composites

Laipeng Yan, Zhanqiu Tan, Gang Ji, Zhiqiang Li, Genlian Fan, D. Schryvers, Aidang Shan, Di Zhang

PII: S1044-5803(15)30102-9
DOI: doi: 10.1016/j.matchar.2015.12.031
Reference: MTL 8143

To appear in: *Materials Characterization*

Received date: 28 July 2015
Revised date: 14 December 2015
Accepted date: 27 December 2015

Please cite this article as: Yan Laipeng, Tan Zhanqiu, Ji Gang, Li Zhiqiang, Fan Genlian, Schryvers D, Shan Aidang, Zhang Di, A quantitative method to characterize the Al_4C_3-formed interfacial reaction: the case study of MWCNT/Al composites, *Materials Characterization* (2015), doi: 10.1016/j.matchar.2015.12.031

This is a PDF file of an unedited manuscript that has been accepted for publication. As a service to our customers we are providing this early version of the manuscript. The manuscript will undergo copyediting, typesetting, and review of the resulting proof before it is published in its final form. Please note that during the production process errors may be discovered which could affect the content, and all legal disclaimers that apply to the journal pertain.

ACCEPTED MANUSCRIPT

A quantitative method to characterize the Al_4C_3-formed interfacial reaction: the case study of MWCNT/Al composites

Laipeng Yan [a], Zhanqiu Tan [a], Gang Ji [b], Zhiqiang Li [a, *], Genlian Fan [a], D. Schryvers [c], Aidang Shan [d,e], Di Zhang [a]

[a] State Key Laboratory of Metal Matrix Composites, Shanghai Jiao Tong University, Shanghai 200240, China

[b] Unité Matériaux et Transformations (UMET), CNRS UMR 8207, Université Lille 1, 59655 Villeneuve d'Ascq, France

[c] Electron Microscopy for Materials Science (EMAT), University of Antwerp Groenenborgerlaan 171, 2020 Antwerp, Belgium

[d] School of Materials Science and Engineering, Shanghai Jiao Tong University, Shanghai 200240, China

[e] School of Environmental Science and Engineering, Shanghai Jiao Tong University, Shanghai 200240, China

Abstract

The Al_4C_3-formed interfacial reaction plays an important role in tuning the mechanical and thermal properties of carbon/aluminum (C/Al) composites reinforced with carbonaceous materials such as multi-wall carbon nanotube (MWCNT) and graphene nanosheet. In terms of the hydrolysis nature of Al_4C_3, an electrochemical dissolution method was developed to quantitatively characterize the extent of C/Al interfacial reaction, which involves dissolving the composite samples in alkaline solution first, then collecting and measuring the CH_4 gas released by Al_4C_3 hydrolysis with a gas chromatograph. Through a case study with powder metallurgy fabricated 2.0 wt.% MWCNT/Al composites, the detectability limit of the proposed method is 0.4 wt.% Al_4C_3, corresponding to 5 % extent of interfacial reaction with a measurement error of ± 3 %. And then, with the already known MWCNT/Al reaction extent vs different sintering temperature and time, the reaction kinetics with an activation energy of 281 kJ mol^{-1} was successfully derived. Therefore, this rapid, sensitive, accurate method supplies an useful tool to optimize the processing and properties of all kinds of C/Al composites via interface design/control.

* Corresponding author. Tel.: +86 21 5474 5872. Fax: +86 21 3420 2749
E-mail address: lizhq@sjtu.edu.cn (Z. Li) , tanzhanqiu@sjtu.edu.cn (Z. Tan).

ACCEPTED MANUSCRIPT

Keywords: MWCNT/Al composite; Interfacial reaction; Aluminum carbide; Electrochemical dissolution.

1. Introduction

Carbon/Aluminum (C/Al) composites reinforced with carbonaceous materials such as multi-wall carbon nanotube (MWCNT), graphene nanosheet, carbon fiber, diamond/graphite particle, are promising candidates for next-generation metallic composites due to their excellent mechanical and thermal properties [1-6]. In addition to the spatial distribution of the reinforcements, the interfacial configurations, including chemistry, structure and bonding, also play an important role in determining the global properties of all kinds of the C/Al composites [7-9]. An ideal C/Al interface should not only transfer the applied load from the matrix to the reinforcements, but also facilitate the thermal exchange by reducing the interfacial thermal resistance [10-12]. In fact, the chemical reaction between Al matrix and carbonaceous reinforcements, in terms of the equation $4Al+3C \rightarrow Al_4C_3$, is thermodynamically favorable both in casting and powder metallurgy processing routes. Many literatures reported that the formation of a ceramic Al_4C_3 phase at the C/Al interface can improve interfacial bonding to some extent [13, 14]. However, the formation of excessive Al_4C_3 is considered to be harmful due to its intrinsic brittleness, low thermal conductivity and strong tendency of hydrolysis [15, 16]. In other words, the properties and reliability of the C/Al composites significantly depend on the extent of the Al_4C_3-formed interfacial reaction. Therefore, it becomes a critical issue to correlate the properties with various processing conditions and interfacial reaction extent.

ACCEPTED MANUSCRIPT

But it is embarrassing that so far there is no efficient, quantitative method to evaluate the extent of C/Al interfacial reaction. Usually, the Al_4C_3 resulted from interfacial reaction has been characterized either by X-ray diffraction (XRD) and Raman spectroscopy (RS), or by scanning electron microscopy (SEM) and transmission electron microscopy (TEM) [17]. XRD and RS are semi-quantitative methods and can only be used to detect Al_4C_3 when its content is higher than 4-5 wt.%. Comparatively, SEM and TEM allow one to directly observe the morphology of Al_4C_3 product, but there is no statistical significance considering the localized, limited field of view in SEM and TEM. In this regard, Lee *et al.* [18] and Monje *et al.* [19] attempted to extract the Al_4C_3 particles from SiC/Al and diamond/Al composites by electrochemically dissolving the Al matrix, and then gave a qualitative comparison of the interfacial reaction extent by direct SEM observation. Hence, none of the above-mentioned techniques are viable for quantitatively measuring the amount of Al_4C_3 formed in the C/Al composites.

The most feasible method ever reported is to deduce the content of Al_4C_3 from the amount of methane (CH_4) released from the hydrolysis of Al_4C_3 [15]. This method involved dissolving diamond/Al sample (~0.5 g) in a 20 % HCl solution and then analytically measured the CH_4 collection by a gas chromatograph [15]. This chemical dissolution-gas chromatography method supplied a possible solution for quantitatively characterizing the extent of C/Al interfacial reaction. Since no concrete practical experimental set-up was presented in reference [15] and elsewhere, here we have improved this method in the following aspects: (1) Electrochemical dissolution in

ACCEPTED MANUSCRIPT

alkaline solution was used to accelerate the dissolving of C/Al composite samples and the hydrolysis of Al_4C_3; (2) C/Al samples of larger size, e.g. ~1.5 g, was adopted and thus enough CH_4 gas for measurement could be generated in reasonable time. As results, C/Al composites with very low reinforcement content and/or very low interfacial reaction extent could be characterized with reliable accuracy. This is of great importance because our previous studies have demonstrated that in MWCNT/Al [1, 20], diamond/Al [21, 22] and graphite flakes/Al-Si composites [23], better mechanical and thermal properties always occur with very low Al_4C_3 content. As a case study, powder metallurgy fabricated 2.0 wt.% MWCNT/Al composites have been used to validate the newly developed method. The detectability limit (i.e. the minimum reaction extent could be detected) and accuracy were shown to be around 5 % and $\pm$3 %, respectively, which were far beyond the ability of XRD and RS.

2. Material and methods

Aluminum powders (99.9 % in purity) with an average particle size of 30 μm were used as the matrix material. MWCNTs (99.9 % in purity) of about 150 nm in diameter and of 10~20 μm in length were used as the reinforcement. The mass fraction of MWCNTs in the composites was 2.0 wt.%. MWCNTs and Al powders were first mechanically mixed and then ball milled for 3 h, with a ball-to-powder weight ratio of 20:1 and a milling speed of 352 rpm, to uniformly disperse MWCNTs on the surface of Al flakes as obtained. Then, the MWCNT/Al composite powders were cold pressed into a cylinder of 40 mm in diameter by uniaxial pressure of 350 MPa. Subsequently, the green billets were sintered in a vacuum hot pressing (VHP)

ACCEPTED MANUSCRIPT

unit with a graphite mold. The VHP process involved the following steps: (1) the billets were heated up to 400 °C at the rate of 10 °C/min and then held for 0.5 h for degassing; (2) the billets were further heated up to temperatures range of 570-640 °C and then held for 0.5-6.0 h to induce different interfacial reaction extent, while a uniaxial pressure of 67.7 MPa was applied to promote the consolidation of MWCNT/Al composites according to the previous works [6, 21, 22]. After furnace cooling, the sintered billets were cut into 15×15×2.5 mm plate samples, polished and then cleaned in an ultrasonic cleaner to remove impurities on the surface.

The VHPed MWCNT/Al samples were characterized by the newly developed method (see 3.1 for details) as well as XRD, RS and TEM for comparison. XRD was performed on an X-Ray diffractometer (XRD-6100, Shimadzu Co. Ltd., Japan), operating at 40 kV/40 mA and using Cu K_α radiation (λ=0.15406 nm). 2θ scans were performed between 20 and 90° with a scan speed of 5°/min. Careful scanning was performed in the angle range of 30-37° with a step size of 0.01° and scan time of 2 s per increment to check the presence of Al_4C_3 (JCPDS file 35-0799). Raman spectra were recorded with a microscopic laser Raman spectrometer (Senterra R200-L, Bruker Co. Ltd, German) in the back-scattering geometry, and by using the 532 nm line of a diode-pumped solid-state laser in the spectral range from 400 to 2000 cm^{-1}. An FEI Tecnai G2 transmission electron microscope, operated at 200 kV and equipped with an EDAX energy-dispersive X-ray spectrometry (EDX) detector, was used for high-resolution (HR) TEM characterization. EDX spectrum was recorded in TEM mode by using a focused beam having the size of a few nanometers. TEM thin

ACCEPTED MANUSCRIPT

foils were prepared by mechanical polishing to reduce sample thickness down to around 30-50 μm. Final ion milling of punched disk samples, having 3 mm in diameter, was carried out by using a Gatan Model 691 precision ion polishing system. Accelerating voltage was set to 5 kV and dual ion sources with milling angles of 10° was employed. Total ion milling time was in the range 2-3 h to reach electron transparency.

3. Results and discussion

3.1. The experimental set-up and quantitative characterization method

The newly developed method mainly includes three steps: electrochemical dissolution, gas collection and gas chromatography analysis. As shown in Fig. 1, the measurement is conducted in completely airtight environment using a deliberately designed experimental set-up that integrates separating funnel, sealing flange and electrodes from top to bottom (see Fig. 1b), which is convenient for injecting and draining the electrochemical electrolyte. Sodium hydroxide (NaOH) aqueous solution with a concentration of 4 mol/L is used as the electrolyte and its quantity is adjusted by the separating funnel. Instead of chemical dissolution initially proposed in [15], electrochemical dissolution has been used in order to accelerate the dissolving of the samples. Current density of 2 A/cm^2 is controlled by a direct current power supply (PS405D). As can be seen in Table 1, it enables the dissolution speed nearly one order of magnitude higher than chemical dissolution. Within 1.0-5.0 h, the sintered MWCNT/Al samples (~1.5 g each) could be completely dissolved in the NaOH

ACCEPTED MANUSCRIPT

solution while the released CH_4 is purged with pure nitrogen gas. The CH_4/N_2 is collected in a vacuum bag, and after digestion, injected with a fixed amount (50 ml) of CO gas as a reference for subsequent analysis. Then the gas mixture is passed through a gas chromatograph (GC-2010, Shimadzu Co. Ltd, Japan), which can quantitatively measure the concentration of CH_4 and CO.

The reactions during the electrochemical dissolution of C/Al composites are listed as follows.

$$2Al\text{-}6e^- \rightarrow 2Al^{3+} \quad (1)$$

$$6H^+ + 6e^- \rightarrow 3H_2 \quad (2)$$

$$Al_4C_3 + 4H_2O + 4OH^{-1} \rightarrow 4AlO_2^- + 3CH_4 \uparrow \quad (3)$$

According to equation (3), whatever the C/Al composites are, only Al_4C_3 can react with water to generate CH_4 gas. Thus the reacted carbon, namely the absolute mass of C in Al_4C_3 or CH_4 can be calculated by the volume of CH_4 released by Al_4C_3 hydrolysis.

$$m_{C-Al_4C_3} = m_{C-CH_4} = 12 \times V_{CH4} / 22.4 \quad (4)$$

If we define the extent of interfacial reaction, η, as the mass ratio of reacted carbon to total carbon in C/Al samples, then it can be deduced from formula (5).

$$\eta = \frac{m_{C-Al_4C_3}}{m_{C-C/Al}} \times 100\% = \frac{12 \times V_{CH_4} / 22.4}{m_{C/Al} \times w} \times 100\% \quad (5)$$

Where V_{CH_4} is the volume of CH_4, $m_{C-Al_4C_3}$ and $m_{C-C/Al}$ are the mass of C in Al_4C_3 and C/Al sample, respectively. While $m_{C/Al}$ is the mass of C/Al sample, ω is the

ACCEPTED MANUSCRIPT

mass fraction of C in C/Al sample, which is measured by a carbon sulfur infrared spectrometer (CSI, CS-206, BaoYing Tech, China).

The interfacial reaction extent of different MWCNT/Al samples is calculated based on formula (5) and the results are plotted in Fig. 2. As expected, the interfacial reaction extent increases with sintering temperature and sintering time.

It was reported that the solubility of CH_4 in 4 mol/L NaOH aqueous solution was about 0.64 mg/100 g at 60 $^{\circ}$C [24, 25]. In our case, the possible mass of CH_4 released by the 2.0 wt.% MWCNT/Al (~1.5 g) samples is in the range 0-40 mg. Hence, the measurement error could be caused by residual CH_4 dissolved in the aqueous solution and/or CH_4 remained within connecting conduct, particular in the case of very low Al_4C_3 content (e.g. the 570°C-2h sample shown in Fig. 2). To reduce the measurement error, the experimental set-up was carefully purged with nitrogen gas after electrochemical dissolution, and the purging gas was collected in the vacuum bag for measurement.

3.2. Al_4C_3 content characterization and comparison with XRD, RS and TEM

Sintering temperature and time are two main factors determining the extent of the Al_4C_3-formed interfacial reaction. Higher sintering temperature and longer time always result in more severe reaction [26]. As shown in Fig. 3a, Al (111), (200), (220), (311) and (222) peaks are clearly visible for all the MWCNT/Al samples. Because the content of MWCNTs (2.0 wt.%) and Al_4C_3 (8.0 wt.% if all the MWCNTs be converted) may be less than the detectability limit of XRD, no C peaks and Al_4C_3

ACCEPTED MANUSCRIPT

peaks are detected by XRD except for in the sample sintered at the highest sintering temperature for the longest time, i.e. at 640 °C for 5 h. As shown in Fig. 3b, the Al_4C_3 (101), (012), (009) and (015) peaks only appear in the 640 °C-5 h sample, which corresponds to a very high extent (91%) of interfacial reaction, namely 0.1092 g Al_4C_3 (~7.3 wt.%) is formed according to the proposed quantitative method. Similarly, RS peaks of Al_4C_3 (494 and 868 cm^{-1}) are clearly visible only in the 640 °C-5 h sample. For the samples of lower interfacial reaction extent, however, the RS peaks of MWCNTs display notable broadening/shift in both D-band (1350 cm^{-1}) and G-band (1585 cm^{-1}) which may suggests the amorphization of MWCNTs and the transformation into Al_4C_3 with the increased sintering temperature and time [17, 27]. Typically, the D-band becomes stronger while the G-band becomes weaker after sintering. As a result, the I_D/I_G ratio increases from 0.46 (MWCNT/Al powders) to 1.08 (570 °C-2 h sample), which indicates the accumulation of structural defects in MWCNTs [27]. Besides, the shift of G-band toward higher frequencies (see in Fig.4a) indicates the amorphization of MWCNTs as reported earlier [17, 27]. Hence, Neither XRD nor RS are suitable for evaluation of low interfacial reaction extent with very low Al_4C_3 content, such as in the case of MWCNT/Al samples sintered at 570 °C, 600 °C and 640 °C for 2 h.

As evidenced above, XRD (Fig. 3) and RS (Fig. 4) have poor measurement accuracy and can only be used in the case of a quite high Al_4C_3 content, such as the 640 °C-5h sample that contains ~7.3 wt.% Al_4C_3. But when the interfacial reaction extent is quite low such as 5 % in the 600°C-0.5h sample, conventional techniques

ACCEPTED MANUSCRIPT

like XRD and RS fail to give reasonable results. In contrast to XRD and RS, the proposed quantitative method can detect Al_4C_3 content as low as 0.4 wt.%, namely 0.006 g Al_4C_3 formed in the 600°C-0.5h sample ~1.5 g in weight, as shown in Fig. 2b. This means that the detectability limit, i.e. the minimum reaction extent could be detected by the proposed quantitative method is 5 %, with a measurement error of ±3 % determined by doing the same test for 5 times.

Furthermore, the validity of the proposed quantitative method have been verified by TEM observation. The exemplified TEM results obtained from the 570°C-2h and 640°C-5h (for comparison) samples are shown in Fig. 5. In general, the contrast of the Al_4C_3 phase is dependent on its orientation with respect to the incident electron beam. By extensive sample tilting in the angle range of ± 30° (tilting limits of our microscope), only five needle-like and/or plate-like morphologies are identified in the 570°C-2h sample (arrowed in Fig. 5a), which can correspond to Al_4C_3. A plate-like Al_4C_3 oriented to the [100] direction is further confirmed by HRTEM (Fig. 5c) and EDX (Figs. 5e-g). In the same sample as shown in Fig. 5d, two complete MWCNTs are locally conserved and no interfacial Al_4C_3 is visible at the MWCNT/Al interfaces at this scale. Comparatively, a large amount of needle-like and plate-like Al_4C_3 compounds are present in Fig. 5b (640°C-6h) having the field of view with the same magnification as in Fig. 5a. Hence, it is confirmed by TEM that the quantitative method remains effective in the range of very low Al_4C_3 content, where XRD and RS become invalid.

Finally, the proposed quantitative method also provides access to the kinetics and

ACCEPTED MANUSCRIPT

reaction activation energy of the Al_4C_3-formed interfacial reaction. Based on parabolic law [28]:

$$dw/dt = K/w \tag{6}$$

$$w^2/2 = Kt + C \tag{7}$$

Considering w=0 when t=0:

$$w = (2Kt)^{1/2} \tag{8}$$

where *w*, *K* and *t* are the weight of Al_4C_3, the growth rate constant and the holding time in sintering process, respectively. Moreover, the growth rate constants at different temperatures allow to estimate the activation energy by using subsequent Arrhenius' law [28]

$$K = k\exp(-Q/RT) \tag{9}$$

$$\ln(2K)^{1/2} = \ln(2k)/2 - Q/(2RT) \tag{10}$$

where *k*, *Q*, and *R* are the constant, activation energy (kJ mol^{-1}) and gas constant (8.314 K^{-1} mol^{-1}), respectively. The activation energy is calculated from the gradient of the linear fitting line in a graph of $\ln(2K)^{1/2}$ versus $1/(2RT)$.

As plotted in Fig. 6a, the gradients of the linear fitting lines $(2K)^{1/2}$ are 0.1406, 0.4457 and 0.6752 at different sintering temperatures of 570, 600 and 640°C, respectively. The three growth rate constants are then expressed in an Arrhenius plot as shown in Fig. 6b. From the gradient of this plot, the activation energy *Q* is determined to be around 281 kJ mol^{-1}, which is different from the previously reported

ACCEPTED MANUSCRIPT

values of 230 kJ mol^{-1} for the C/Al (or Al alloys) [29], 448 kJ mol^{-1} for the AlN/Al-C [30] and 349 kJ mol^{-1} for the C_{fiber}/Al [31], due to the difference in structural integrity and surface defect concentration in different composite systems.

As we know, the milling process may introduce extra structural defects to MWCNTs [32], which makes them more susceptible to react with the Al matrix and leads to a low activation energy. Ci *et al.* [26] have revealed that the MWCNT/Al interfacial reaction occurs stage by stage due to the special structure of MWCNTs. In the first stage, the C atoms at the cap or defect sites preferentially react with Al, and the Al_4C_3 can nucleate at these defect places even at a temperature lower than 500 °C. In the second stage, following the consumption of C atoms at the cap or defect sites, the C atoms elsewhere will diffuse through Al matrix towards the nucleus, and then Al_4C_3 begin to grow and coarsen. Thus, the value of 281 kJ mol^{-1} calculated in this study should be the apparent activation energy in related with these two stages.

4. Summary and conclusions

Although the underlying role of C/Al interfacial reaction and resulted Al_4C_3 is still unclear, it has been proved to be a feasible pathway to tailoring the properties of aluminum composites reinforced with carbon nanotube, graphene nanosheet, carbon fiber, diamond/graphite particle. Regarding this, we have developed a method of electrochemical dissolution-CH_4 gas collection-gas chromatography to quantitatively characterize the extent of C/Al interfacial reaction in terms of the Al_4C_3 amount formed in the composite. The VHPed MWCNT/Al composites with different Al_4C_3 content have been used to validate the effectiveness of this method. As confirmed by

ACCEPTED MANUSCRIPT

XRD, RS and TEM, the detectability limit of this method is around 5 % with an accuracy of ±3 %. And then, with the already known MWCNT/Al interfacial reaction extent vs different sintering temperature/time, the reaction kinetics with an activation energy of 281 kJ mol^{-1} was derived. Therefore, the proposed quantitative method supplies a useful tool to optimize the processing and properties of all kinds of C/Al composites via interface design and control, which is a key research area worthy of further in-depth study.

Acknowledgements

The authors would like to acknowledge the financial support of the National Basic Research Program of China (973 Program, No. 2012CB619600), the National High-Tech R&D Program (863 Program, No. 2012AA030611), the National Natural Science Foundation (Nos. 51071100, 51131004, 51401123, 51511130038) and the research grant (Nos. 14DZ2261200, 15JC1402100, 14520710100) from Shanghai government. Dr. Z.Q. Tan would also like to thank the project funded by the China Postdoctoral Science Foundation (No. 2014M561469). The research leading to these results has partially received funding from the European Union Seventh Framework Program under Grant Agreement 312483 - ESTEEM2 (Integrated Infrastructure Initiative - I3).

References

[1] L. Jiang, Z.Q. Li, G.L. Fan, L.L. Cao, D. Zhang, Strong and ductile carbon

ACCEPTED MANUSCRIPT

nanotube/aluminum bulk nanolaminated composites with two-dimensional alignment of carbon nanotubes, Scripta Mater, 66 (2012) 331-334.

[2] K. Chu, C.C. Jia, W.H. Tian, X.B. Liang, H. Chen, H. Guo, Thermal conductivity of spark plasma sintering consolidated SiCp/Al composites containing pores: Numerical study and experimental validation, Compos Part A, 41 (2010) 161-167.

[3] S.F. Bartolucci, J. Paras, M.A. Rafiee, J. Rafiee, S. Lee, D. Kapoor, N. Koratkar, Graphene–aluminum nanocomposites, Mater Sci Eng: A, 528 (2011) 7933-7937.

[4] H. Naji, S.M. Zebarjad, S.A. Sajjadi, The effects of volume percent and aspect ratio of carbon fiber on fracture toughness of reinforced aluminum matrix composites, Mater Sci Eng: A, 486 (2008) 413-420.

[5] J. Chen, I. Huang, Thermal properties of aluminum–graphite composites by powder metallurgy, Compos Part B, 44 (2013) 698-703.

[6] Z. Tan, Z. Li, G. Fan, Q. Guo, X. Kai, G. Ji, L. Zhang, D. Zhang, Enhanced thermal conductivity in diamond/aluminum composites with a tungsten interface nanolayer, Mater Design, 47 (2013) 160-166.

[7] S.R. Bakshi, A. Agarwal, An analysis of the factors affecting strengthening in carbon nanotube reinforced aluminum composites, Carbon, 49 (2011) 533-544.

[8] S.R. Bakshi, A.K. Keshri, V. Singh, S. Seal, A. Agarwal, Interface in carbon nanotube reinforced aluminum silicon composites: Thermodynamic analysis and experimental verification, J Alloy Compd, 481 (2009) 207-213.

[9] A. Esawi, K. Morsi, A. Sayed, M. Taher, S. Lanka, The influence of carbon nanotube (CNT) morphology and diameter on the processing and properties of

ACCEPTED MANUSCRIPT

CNT-reinforced aluminium composites, Compos Part A, 42 (2011) 234-243.

[10] T. Laha, S. Kuchibhatla, S. Seal, W. Li, A. Agarwal, Interfacial phenomena in thermally sprayed multiwalled carbon nanotube reinforced aluminum nanocomposite, Acta Mater, 55 (2007) 1059-1066.

[11] S.R. Bakshi, A.K. Keshri, V. Singh, S. Seal, A. Agarwal, Interface in carbon nanotube reinforced aluminum silicon composites: Thermodynamic analysis and experimental verification, J Alloy Compd, 481 (2009) 207-213.

[12] R. Andrews, M. Weisenberger, Carbon nanotube polymer composites, Curr Opin Solid St M, 8 (2004) 31-37.

[13] A. Desai, M. Haque, Mechanics of the interface for carbon nanotube–polymer composites, Thin Wall struct, 43 (2005) 1787-1803.

[14] D.B. Miracle, S.L. Donaldson, S.D. Henry, C. Moosbrugger, G.J. Anton, B.R. Sanders, N. Hrivnak, C. Terman, J. Kinson, K. Muldoon, ASM handbook, ASM International Materials Park, OH, USA, 2001.

[15] W.B. Johnson, B. Sonuparlak, Diamond/Al metal matrix composites formed by the pressureless metal infiltration process, J Mater Res, 8 (1993) 1169-1173.

[16] M. Rodriguez-Reyes, M. Pech-Canul, J. Parga-Torres, J. Acevedo-Davila, M. Sanchez-Araiza, H. Lopez, Development of aluminum hydroxides in Al–Mg–Si/SiC p in infiltrated composites exposed to moist air, Ceram Int, 37 (2011) 2719-2722.

[17] B. Chen, L. Jia, S. Li, H. Imai, M. Takahashi, K. Kondoh, In Situ Synthesized Al_4C_3 Nanorods with Excellent Strengthening Effect in Aluminum Matrix Composites, Adv Eng Mater, 16 (2014) 972-975.

ACCEPTED MANUSCRIPT

[18] J. Lee, J.-I. Lee, H.-I. Lee, Observation of three-dimensional interfacial morphologies in SiC_p/Al composites and its characterization, J Mater Sci Lett, 15 (1996) 1539-1542.

[19] I.E. Monje, E. Louis, J.M. Molina, Aluminum/diamond composites: A preparative method to characterize reactivity and selectivity at the interface, Scripta Mater, 66 (2012) 789-792.

[20] H. Wei, Z. Li, D.-B. Xiong, Z. Tan, G. Fan, Z. Qin, D. Zhang, Towards strong and stiff carbon nanotube-reinforced high-strength aluminum alloy composites through a microlaminated architecture design, Scripta Mater, 75 (2014) 30-33.

[21] Z. Tan, Z. Li, G. Fan, X. Kai, G. Ji, L. Zhang, D. Zhang, Diamond/aluminum composites processed by vacuum hot pressing: microstructure characteristics and thermal properties, Diam Relat Mater, 31 (2013) 1-5.

[22] Z. Tan, Z. Li, G. Fan, X. Kai, G. Ji, L. Zhang, D. Zhang, Fabrication of diamond/aluminum composites by vacuum hot pressing: process optimization and thermal properties, Compos Part B, 47 (2013) 173-180.

[23] C. Zhou, G. Ji, Z. Chen, M. Wang, A. Addad, D. Schryvers, H. Wang, Fabrication, interface characterization and modeling of oriented graphite flakes/Si/Al composites for thermal management applications, Mater Design, 63 (2014) 719-728.

[24] Z. Duan, N. Møller, J. Greenberg, J.H. Weare, The prediction of methane solubility in natural waters to high ionic strength from 0 to 250 C and from 0 to 1600 bar, Geochim Cosmochim Ac, 56 (1992) 1451-1460.

[25] Z. Duan, S. Mao, A thermodynamic model for calculating methane solubility,

ACCEPTED MANUSCRIPT

density and gas phase composition of methane-bearing aqueous fluids from 273 to 523K and from 1 to 2000bar, Geochim Cosmochim Ac, 70 (2006) 3369-3386.

[26] L. Ci, Z. Ryu, N.Y. Jin-Phillipp, M. Rühle, Investigation of the interfacial reaction between multi-walled carbon nanotubes and aluminum, Acta Mater, 54 (2006) 5367-5375.

[27] D. Poirier, R. Gauvin, R.A. Drew, Structural characterization of a mechanically milled carbon nanotube/aluminum mixture, Compo Part A, 40 (2009) 1482-1489.

[28] A. Okura, K. Motoki, Rate of formation of intermetallic compounds in aluminium matrix-carbon fibre composites, Compos Sci Technol, 24 (1985) 243-252.

[29] K. Landry, S. Kalogeropoulou, N. Eustathopoulos, Wettability of carbon by aluminum and aluminum alloys, Mater Sci Eng: A, 254 (1998) 99-111.

[30] C. Toy, W. Scott, Wetting and spreading of molten aluminium against AlN surfaces, J Mater Sci, 32 (1997) 3243-3248.

[31] M. Lee, Y. Choi, K. Sugio, K. Matsugi, G. Sasaki, Effect of aluminum carbide on thermal conductivity of the unidirectional CF/Al composites fabricated by low pressure infiltration process, Compos Sci Technol, 97 (2014) 1-5.

[32] M.T. Hassan, A.M. Esawi, S. Metwalli, Effect of carbon nanotube damage on the mechanical properties of aluminium–carbon nanotube composites, J Alloy Compd, 607 (2014) 215-222.

ACCEPTED MANUSCRIPT

Table Captions

Table 1 Time consumption to dissolve MWCNT/Al samples (~1.5 g each)

ACCEPTED MANUSCRIPT

ACCEPTED MANUSCRIPT

Figure Captions

Fig. 1 (a) Schematic diagram and (b) the experimental set-up developed in this work.

Fig. 2 Extent of interfacial reaction measured by the newly developed method in 2.0 wt.% MWCNT/Al samples ~1.5 g in weight: (a) sintered at different temperature and for different time; (b) sintered at 600 °C but for different times (0.5-6.0 h). The weight of the reaction-formed Al4C3 is given above each data. Note that each data is an average of five measurements and the measurement error is ±3 %.

Fig. 3 (a) XRD patterns of the MWCNT/Al composites sintered at different conditions as shown in Fig. 2(a); (b) careful scanning XRD traces in the angle range of 30-37° to highlight the (101), (012), (009) and (015) diffraction peaks of the formed Al_4C_3 phase.

Fig. 4 (a) Raman spectra of the MWCNT/Al composites sintered at different conditions as shown in Fig. 2(a) and Fig. 3(a); (b) Raman spectra of the MWCNT/Al composites sintered at 600 °C for different times as shown in Fig. 2b. Note that the peaks of D- and G-bands correspond to MWCNTs.

Fig. 5 TEM bright-field images of the MWCNT/Al composites: (a) sintered at 570 °C for 2h; (b) sintered at 640 °C for 5h; (c) HRTEM image of the Al_4C_3 compound in the box shown in (a), inset is the FFT pattern corresponding to the [100] Al_4C_3 orientation; (d) TEM bright-field image of the MWCNT/Al interfaces, inset is the electron diffraction pattern of the MWCNT; (e)-(g) typical EDX spectra of Al_4C_3, MWCNT,

ACCEPTED MANUSCRIPT

Al matrix. Arrows in (a) and (b) note the needle-like and plate-like Al_4C_3.

Fig. 6 (a) The amount of reaction-formed Al_4C_3 as a function of sintering time at different sintering temperatures of 570, 600 and 640 °C, and (b) the calculated growth constant as a function of sintering temperature to determine the reaction activation energy (see text for more details).

ACCEPTED MANUSCRIPT

ACCEPTED MANUSCRIPT

Table 1

Method	Chemical dissolution	Electrochemical dissolution			
Current density (A/cm^2)	0	1	2	3	4
Time (h)	25	5	2	1.5	1

ACCEPTED MANUSCRIPT

ACCEPTED MANUSCRIPT

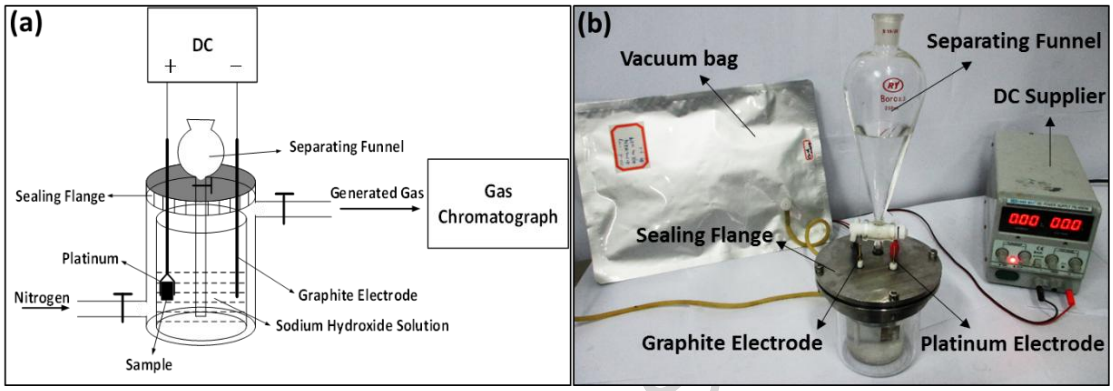

Fig. 1

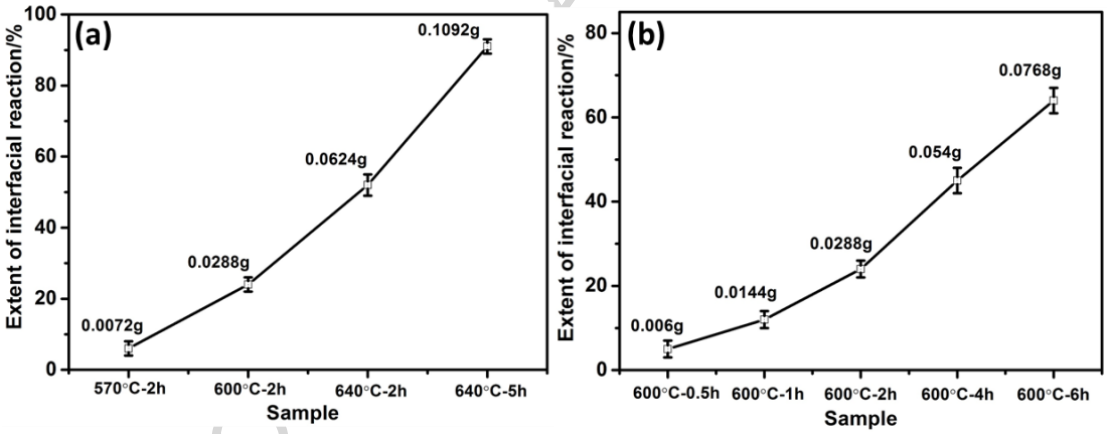

Fig. 2

ACCEPTED MANUSCRIPT

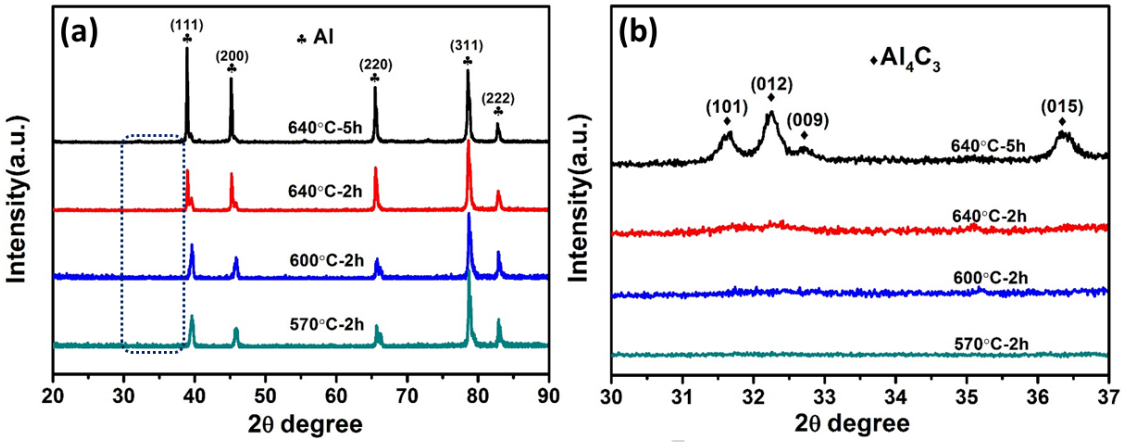

Fig. 3

ACCEPTED MANUSCRIPT

ACCEPTED MANUSCRIPT

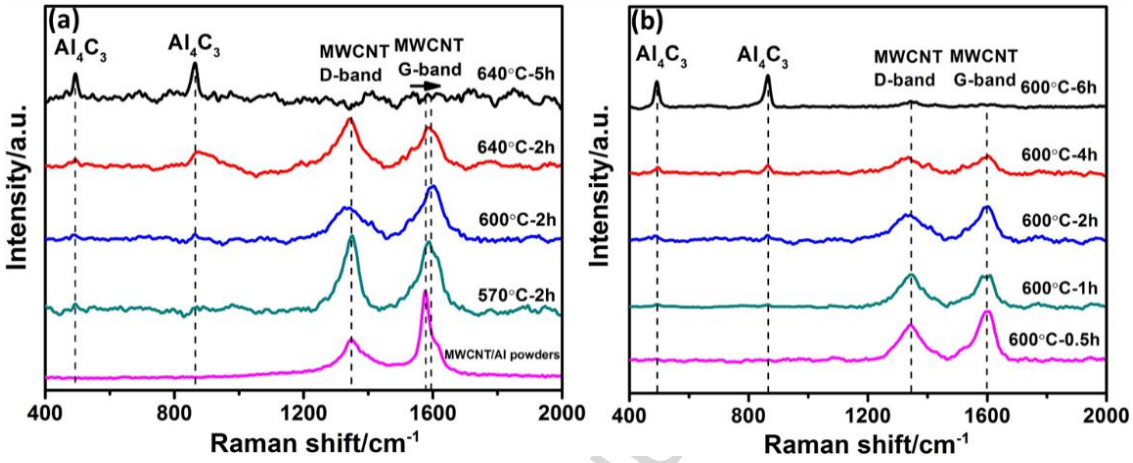

Fig. 4

ACCEPTED MANUSCRIPT

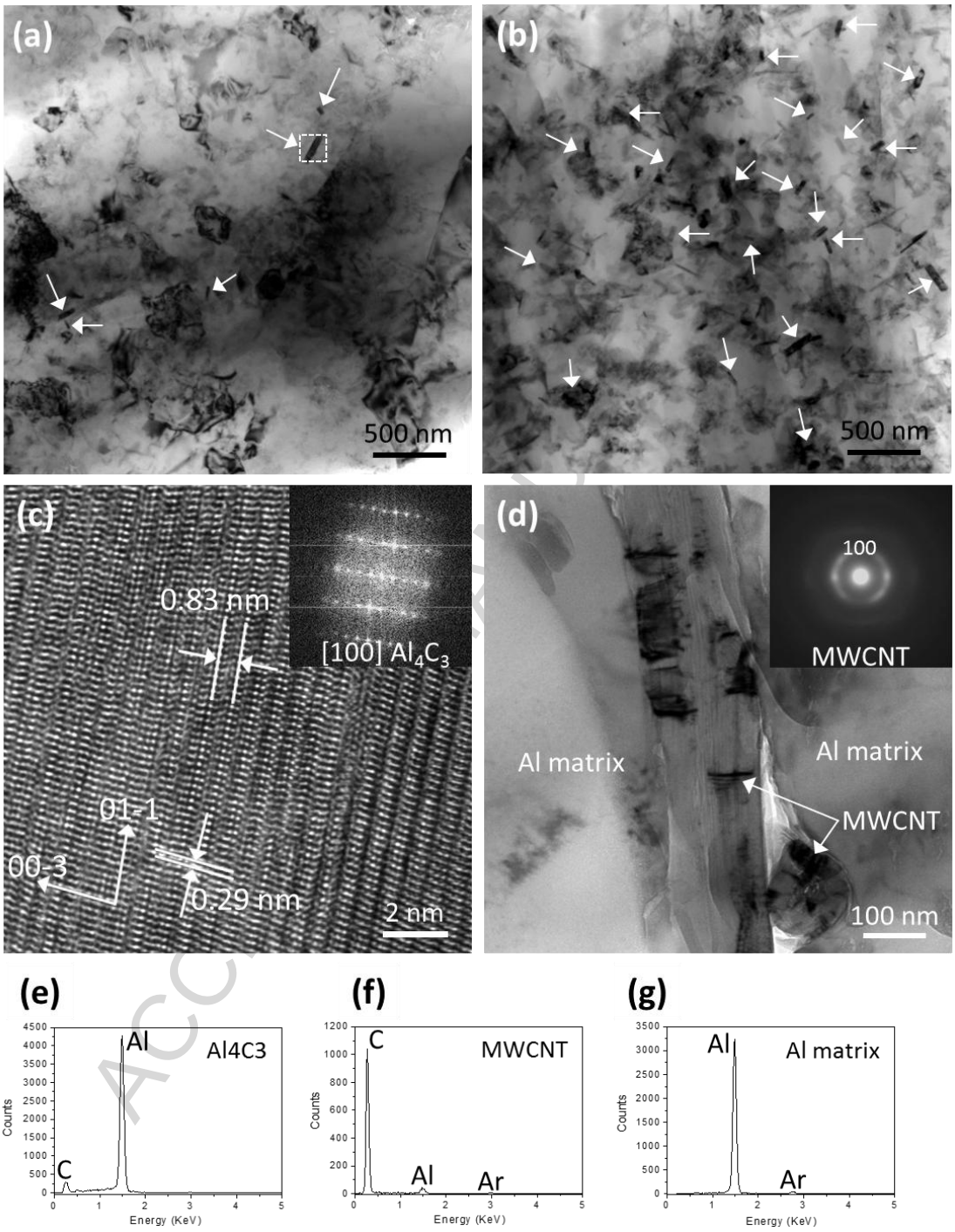
(a)
500 nm
(b)
500 nm
(c)
0.83 nm
[100] Al_4C_3
01-1
00-3
0.29 nm
2 nm
(d)
100
MWCNT
Al matrix
Al matrix
MWCNT
100 nm
(e)
Al
Al4C3
C
Counts
Energy (KeV)
(f)
C
MWCNT
Al
Ar
Counts
Energy (KeV)
(g)
Al
Al matrix
Ar
Counts
Energy (KeV)

Fig. 5

ACCEPTED MANUSCRIPT

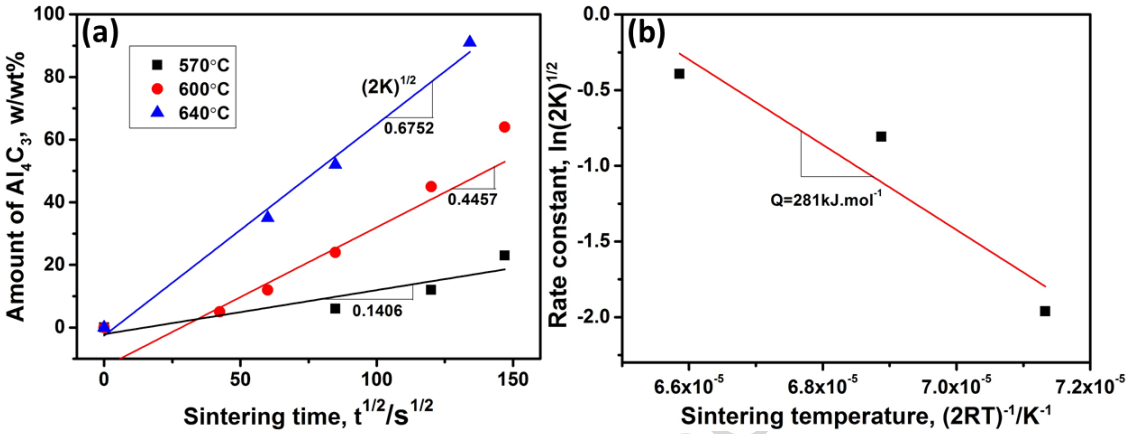

Fig. 6

ACCEPTED MANUSCRIPT

ACCEPTED MANUSCRIPT

Highlights

- A quantitative method to test interfacial reaction of C/Al composite was developed.
- An in-house set-up for the quantitative method was designed.
- The interfacial evolution of MWCNT/Al composite was characterized.
- The kinetics of MWCNT/Al interfacial reaction was analyzed.

ACCEPTED MANUSCRIPT